# EVALUATION OF AN ELECTRONIC WIND-TUNNEL BALANCE

By

Steven Russell Briggs

# United States
# Naval Postgraduate School


# THESIS

EVALUATION OF AN ELECTRONIC WIND-TUNNEL BALANCE

by

Steven Russell Briggs

Thesis Advisor: Louis V. Schmidt

March 1971

*Approved for public release; distribution unlimited.*

# Evaluation of an Electronic Wind-Tunnel Balance

by

Steven Russell Briggs
Lieutenant Commander, United States Navy
B.S., University of California, Los Angeles, 1963

Submitted in partial fulfillment of the
requirements for the degree of

MASTER OF SCIENCE IN AERONAUTICAL ENGINEERING

from the

NAVAL POSTGRADUATE SCHOOL
March 1971

ABSTRACT

The three-component electronic wind-tunnel balance installed in the 3.5 by 5.0 foot subsonic tunnel of the Aeronautics Department of the Naval Postgraduate School was evaluated for system problem areas. The nonlinear output of the reluctance gage transducers was analyzed and linearized using diode function-generating circuitry. A static calibration was conducted to confirm the linearity of the circuits. Evaluation of the balance system under operating conditions pointed out other areas for future investigation. Aerodynamic support tares must be determined, an improved pitch angle drive system is required, a mechanical damping system should be installed, and the balance must be isolated from its existing elastic platform.

TABLE OF CONTENTS

LIST OF TABLES

LIST OF FIGURES

ACKNOWLEDGEMENTS

The author wishes to thank Professor Louis V. Schmidt, Associate Professor of Aeronautics at the Naval Postgraduate School, for his guidance and support as thesis advisor. The author would also like to express his appreciation to the technicians of the Aeronautics Department associated with this project, in particular Mr. Theodore B. Dunton for his continual assistance.

# I. INTRODUCTION

The three-component electronic wind-tunnel balance installed in the 3.5 by 5.0 foot subsonic tunnel of the Aeronautics Department of the Naval Postgraduate School can be a valuable tool in the education of students. The capability of fast data acquisition and recording will speed up experimental procedures.

This balance was a converted mechanical balance system and one prominent inadequacy disclosed during the conversion precluded its general use. The electrical outputs of the system were nonlinear with respect to increasing loads. This nonlinearity required calibration for all load conditions to produce results. This feature outweighed the favorable aspects of fast data acquisition rate and data recording capability.

The source of the nonlinear load-output relation was finally identified as being due to the reluctance gage transducer. Possible elastic interactions in the balance frame were removed by local stiffening of the structure and careful mechanical alignment. The nonlinearity in the transducer output was corrected by designing a suitable diode function-generator circuit similar in concept to those used in analog computers.

The balance system, like any physical item, will be in a continual state of development. In addition to the nonlinearity problem, other system traits have been identified and suggestions are made for improvement where practicable.

This work was accomplished at the Naval Postgraduate School from June 1970 to March 1971.

## II. ELECTRONIC WIND-TUNNEL BALANCE DESCRIPTION

### A. WIND-TUNNEL BALANCE DESIGNS

Three-component wind-tunnel balances are frequently designed to measure two force components along mutually perpendicular axes and a single moment component about an axis perpendicular to those of the force components. Investigations of longitudinal aerodynamic traits typically include determination of lift and drag forces, and pitching moments.

The ideal balance design allows the simultaneous measurement of all forces and moments, with no interaction between any components. Balances have been successfully designed using a focusing type linkage arrangement similar to a dynafocal engine support system which allows the loads and moments to be measured directly. Proper alignment of such configurations results in only slight interactions taking place. Unfortunately, the balance system treated in this problem was a unique "one-of-a-kind" design and did not lend itself very readily to mechanical readouts without ineractions taking place.

Various techniques of measurement are used. In the past, mechanical methods, such as weight or spring balancing of the applied loads, have been utilized. These methods require considerable time to adjust weights or springs, but have the advantage of incorporating mechanical dampers to average the loads when oscillations occur.

Modern balance systems utilize a load cell to determine the applied forces. The unknown force is applied to the load cell, resulting in a deflection of a bar or ring. This deflection is a direct indication of

the applied load. The load-cell deflection can then produce a measurable electric signal from the transducer, which is related to the load input by a calibration. The measurement of the load-ring deflection is typically accomplished with strain gages. Strain gage installations have a tendency to deteriorate with time, requiring periodic reinstallation of the gages. In addition, the strain gage signal levels are low, thereby requiring much amplification. The calibration of the strain gage is sensitive to power supply voltage.

A disadvantage of an electric readout type of balance is the inherent lack of damping unless such is deliberately provided by mechanical or electrical filtering.

B. BALANCE CONVERSION

In the past, no modern wind-tunnel balance was available at the Naval Postgraduate School. The only balance available was an obsolete mechanical weight balance. The inordinate amount of time and effort required in data collection illustrated the need for a more modern system.

Adequate funds were not available to purchase such a balance, so work was undertaken in early 1967 to convert an existing Task Corporation mechanical balance. The mechanical beam balance weight assembly was removed; however, much of the force resolution linkage was retained, along with the existing model support assembly and vertical support structure.

The linkage that constrained vertical motion and hence sensed lift force was relatively easy to identify. A single load ring was designed to sense lift load. However, the drag force and pitching moment constraints were combined in two horizontal linkage arrays that connected the main vertical balance frame to the support frame at the rear of the balance. The following diagram indicates the linkage arrays.

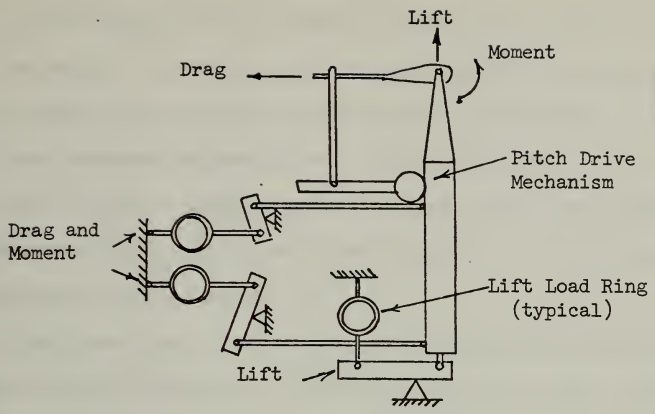


Sketch of Three-Component Balance System

As a result, two load cells were utilized to measure the horizontal linkage loads which were a linear combination of drag and pitching moment.

The three load cells incorporate aluminum rings to react to the applied loads. The resulting ring deflections are sensed by internally mounted Bentley reluctance transducers, yielding a voltage output proportional to diameter change. The reluctance gage was selected because of its durability over time. In addition, the voltage output is more suitable for the ensuing analog circuitry.

The design load range was $\pm$ 500 pounds in lift, 75 pounds in drag, and $\pm$ 150 foot-pounds in moment. The design of the lever arms and load rings insured that the resulting deflection of the rings at design load would be only $\pm$ 0.010 inch for the 3-inch diameter ring with a thickness and width of approximately 0.20 and 0.50 inches, respectively. This principle was selected to maintain linear ring deflections with respect to load.

A Bodine speed reducing motor was installed to provide remote rotation of the model. A ten-turn precision wound potentiometer was geared to the pitch drive and sensed the angle of attack of the model.

The converted balance system is shown in Figure 1.

The reluctance gage and angle of attack outputs are routed through RG58 coaxial cables to a remote control station for signal processing, presentation, and recording.

Operational amplifier circuits provide adjustable gain and zero adjust controls for angle of attack and load cell output. Variable electronic damping circuits are provided for all load cell outputs. An analog summing circuit is provided to separate drag and pitching moment components from the output of load cells two and three.

Chassis outputs from the data processing unit are angle of attack, lift, drag, pitching moment, and two selectable outputs which also provide load cell outputs, both damped and undamped.

The outputs are routed to a Digitec Model 635 scanner. Results are presented on a Digitec Model 251 DC voltmeter and recorded by a Digitec Model 621 printer system. Figure 2 shows all control station components.

It is interesting to note that the initial "breadboard" work on this concept began in 1967 when several students in the Department of Aeronautics started the project as part of a term paper study in an engineering mechanics laboratory. At that time, the operational amplifier circuits used were those available on an EAI Model TR-10 Analog computer.

## C. SYSTEM EVALUATION

The converted balance system represented a great improvement over the existing mechanical balance. The result of the conversion program was an

effective, high speed, electronic balance system capable of automatic data recording.

One prominent undesirable side effect resulted. The voltage output of the system was not linear with respect to applied load. This nonlinearity resulted in the requirement for full range calibration and adjustment of all results. This also prevented use of the drag-moment summing circuits.

In order to improve the balance system, the nonlinearity was identified and corrected.

## III. LINEARIZATION OF LOAD CELL OUTPUTS

### A. IDENTIFICATION OF NONLINEARITY

The original design of the load transmission assemblies and load rings was selected to maintain linear deflection of the rings with respect to load.

In order to identify the source of the nonlinearity, the reluctance gages were removed from the load rings and installed in a Daytronic Model 115A micrometer controlled calibration device (see Figure 3). The original design criterion was a $\pm$ 0.010 inch air gap change for full range deflection. The characteristic output of each transducer and amplifier-driver pair was recorded against air gap over a range of 0.008 to 0.032 inch. The average sensitivity (volts per inch of air gap) of each transducer-driver pair was determined, with typical values being 300 volts per inch. The average transducer output reading at 0.020 inch gap (mid-range) was determined, and a reference voltage reading ($e_{ref}$) was calculated for each air gap setting using the average sensitivity value.

The difference between the voltage output and the reference voltage for each air gap setting was then plotted (Figures 4, 5, and 6). This method was selected in order to accurately identify all slope changes in the resulting plot. The variation of transducer sensitivity over the operating deflection range became obvious, with changes in sensitivity as high as 10.5 per cent noted.

### B. LINEARIZATION TECHNIQUE

Each load cell output versus air gap plot (Figures 4, 5, and 6) was analyzed for the best straight line curve fit. The slope of each segment

of the straight line approximation for each load cell and the break point voltage between individual segments was determined.

The method selected to linearize the signal was the design of diode function generation circuits tailored to each individual load cell requirement. This technique was particularly suited to this task due to the availability of operational amplifiers and a constant voltage source within the existing signal processing circuitry.

1. Diode Function Generating Circuits

The functions required to linearize the load cell output can be generated by using a circuit containing a number of diode-resistor networks.

A typical diode-resistor network utilized in the linearization procedure is:

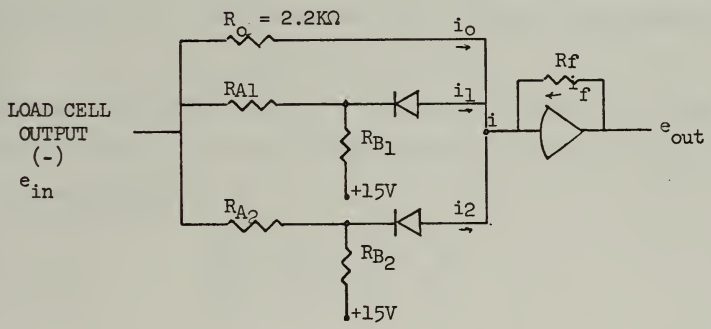


Typical Diode-Resistor Network

The form of the function generated is governed by the selection of the resistors. Resistors $R_{A_n}$ govern changes in the slope, while resistors $R_{B_n}$ govern the location of break points.

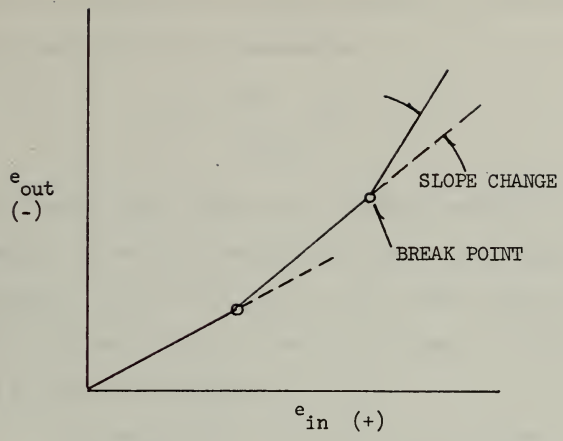


Sample Sensitivity Curve

a. Slope Changes

The slope of each straight line segment was determined. Since at the input to the operational amplifier, Kirkhoff's Law requires that:

$$i = i_0 + i_1 + i_2 = -i_f$$

any change in the resistors $R_{A_n}$ will change the current $i_n$ in that circuit branch. As the base of the operational amplifier is maintained at zero potential:

$$\frac{e_{in}}{R_{net}} = \frac{e_{in}}{R_o} + \frac{e_{in}}{R_1} + \frac{e_{in}}{R_2}$$

or:

$$\frac{1}{R_{net}} = \frac{1}{R_o} + \frac{1}{R_{A_1}} + \frac{1}{R_{A_2}}$$

Typically, for the sum of branches 0 and 1, one obtains;

$$R_{net} = \frac{R_o R_{A_1}}{R_o + R_{A_1}}$$

The gain of an operational amplifier depends upon the values of the feedback and input (net value) resistances.

$$e_o = - \frac{R_f}{R_{net}} e_{in}$$

Thus, the input-output relationship is solely dependent on the ratio of the feedback to the input resistances, plus a sign change.

In order to increase the slope of the output versus air gap relationship, a net decrease in the effective resistance is required, as can be seen by the above relationship.

For example, if it were desired to increase the sensitivity (volts per inch) by ten per cent, then the effective input resistance should be decreased by ten per cent since the amplifier gain is inversely proportional to the effective input load resistance. With a $R_{net}$ of 2.2 kilo-ohms, a decrease of ten per cent, or 1.98 kilo-ohms would be required to effect a ten per cent increase in sensitivity. The required value for an additional resistance in parallel with the existing resistance may be determined by:

$$1.98 = \frac{2.2 \, R_{A_1}}{2.2 + R_{A_1}}$$

$$R_{A_1} = 19.8 \text{ k}\Omega$$

If an increase in the slope were desired, the plate of the diode is placed as noted in the circuit example. In order to decrease the slope, the diode is reversed.

b. Break Points

The breaks in the desired approximating straight line segment are obtained by selection of the resistance $R_{B_n}$.

When the plate of the diode is positive with respect to the cathode, the diode will act as a conductor. If the plate were negative with respect to the cathode, the diode would act as an open switch.

To establish the desired break point, resistance $R_{B_n}$ must be selected to just balance the circuit as:

$$\frac{e_{\text{break point}}}{R_{A_n}} = \frac{15}{R_{B_n}}$$

The end result of the above circuit will be a net change in the sensitivity at the break point. Until the input voltage reaches the break point value, the cathode of the diode will be positive with respect to the plate, thus the diode will act as an open switch. When the break point voltage is exceeded, the diode will conduct, and the resulting parallel circuit will decrease the effective resistance yielding a net increase in the output sensitivity.

If a net decrease in slope (sensitivity) were desired, the diode should be reversed. The diode then conducts until the break point voltage is exceeded. At this point, the branch of the parallel circuit is opened and a net increase in resistance results, hence a net slope decrease occurs.

2. Circuit Linearization Procedures

Each load cell sensitivity curve was first analyzed for initial slope change in the straight line approximation. The required $R_A$ and $R_B$ resistances and diode placement were determined. The circuit was then modeled on a "breadboard" circuit panel. Initial work was accomplished

utilizing an operational amplifier circuit external to the existing signal processing chassis, which proved to be more suitable.

After the temporary calculated circuit was established, re-calibration of each segment was accomplished, with repeat adjustments in $R_A$ and $R_B$ resistances made until the desired straight line slope was achieved.

Throughout the procedure, considerable difficulty was encountered in the selection of diode placement. However, an incorrect choice was immediately noted in the results and easily interpreted. Initial attempts were made to linearize the entire circuit at one time; however, considerable confusion resulted, so the above procedure of single slope changes was adopted.

As each slope change was effectively linearized, the resulting effective resistance was used to calculate resistances required for each succeeding slope change.

When the entire desired range was effectively linearized, final resistance values were measured and the circuits finalized on existing circuit boards for each load cell. Figure 7 shows the final circuits utilized.

After circuit finalization, additional calibration and resistance adjustments were made. Figure 8 presents the final calibration data.

## IV. BALANCE CALIBRATION

The balance was installed beneath the 3.5 by 5.0 foot subsonic wind-tunnel, and the model support struts extended upwards into the test section. A locally manufactured calibration frame using aluminum angle material was installed and aligned in the tunnel test section as presented in Figure 3.

An eccentric cam was installed on an electric motor attached to the balance frame to provide a shaker system to help eliminate friction in the balance linkages and flexures during calibration.

After proper system adjustments, as outlined in Appendix A, each loading condition was investigated utilizing known weights applied in lift, drag, and pitching moment directions. Each component was first calibrated independently, and then mixed loads were applied to confirm calibration accuracies.

The lift calibration results in the positive direction were undependable due to elastic bending of the calibration frame. To circumvent this difficulty, all lift forces were applied in the negative direction, readjusting the transducer on load cell one mechanically to test the circuit over an effective range. The results obtained (Table I) were very satisfactory over a range of $\pm$ 155 pounds, the limit of the calibration system used.

All attempts to isolate drag and pitching moment utilizing the summing circuit failed due to the high gain settings required to obtain desirable readings. As a result, drag and moment settings were calibrated as mixed outputs on load cells two and three. After individual calibrations of drag and moment, sensitivities (pounds of drag per millivolt for

load cell two, etc.) were obtained:

| Component | Sensitivity |
|---|---|
| Drag | -27.666 mv/lb Load Cell 2 |
| | 29.578 mv/lb Load Cell 3 |
| Pitching Moment | -0.8818 mv/inlb Load Cell 2 |
| | 0.4776 mv/inlb Load Cell 3 |

The results of the drag and moment calibration are presented in Table II.

A test of mixed loads of drag and moment produced excellent results (Table III). To isolate drag and moment components from the load cell readings, the following simultaneous equations were used:

$$-27.666\ D - 0.8818\ M = \text{Load Cell 2 (mv)}$$

$$29.578\ D + 0.4776\ M = \text{Load Cell 3 (mv)}$$

The solution of these equations was readily obtained using the programmable Wang Model 360 calculator.

Some minor adjustment in the linearization resistances was required to obtain final results. All linearization resistance potentiometers were placed for easy access through the rear of the signal processing chassis for future re-calibration, if required.

Calibration of the angle of attack system was accomplished with a clinometer placed on the wing calibration template inserted into the levelling plugs. The gain of the angle of attack circuit was adjusted to provide direct read-out of angle of attack. A transverse check from -5 to +15 degrees angle of attack was made to confirm circuit linearity. For future resetting of zero angle of attack, the zero position was referenced to the vernier indicator at the rear of the balance frame.

The results of the balance calibration confirmed the previous results in that the desired linearization had been accomplished over the tested range of:

Lift $\pm$ 155 pounds

Drag + 50 pounds

Moment $\pm$ 480 inch pounds

The criterion for acceptable results was the retention of all zero readings by at most two counts and a variation between lightly and heavily damped readings of two counts. In addition, a one millivolt variation in a reading resulted in a sensitivity of:

$\Delta L = \pm 0.1$ pounds

$\Delta D = \pm 0.06$ pounds

$\Delta M = \pm 1.5$ inch pounds

Tolerances in the dimensionless coefficients for the calibration wing, results of which are presented herein, would be based upon:

$S$ = area = 1.5 square feet

$\bar{c}$ = mean aerodynamic chord = 0.5 feet

$q$ = dynamic pressure = 40.0 pounds per square foot.

Then:

$$\Delta C_D = \frac{\Delta D}{qS} = \pm \frac{0.06 \text{ lbs}}{(40.0 \text{ psf})(1.5 \text{ ft}^2)} = \pm 0.0010$$

$$\Delta C_L = \frac{\Delta L}{qS} = \pm \frac{0.1 \text{ lbs}}{(40.0 \text{ psf})(1.5 \text{ ft}^2)} = \pm 0.0017$$

$$\Delta C_m = \frac{\Delta M}{qS\bar{c}} = \pm \frac{1.5 \text{ inlbs}}{(40.0 \text{ psf})(1.5 \text{ ft}^2)(6.0 \text{ in})} = \pm 0.0040$$

At present, these trends would indicate that the balance is not suitable for accurately measuring aerodynamic properties, since the $\Delta C_D$ sensitivity should be $\pm$ 0.0002, the $\Delta C_L$ sensitivity should be $\pm$ 0.001, and the $\Delta C_m$ sensitivity should be $\pm$ 0.0005. Part of the trouble with resolving drag force and pitching moments is that these readings are obtained by taking differences of two large numbers, with a resultant loss in sensitivity. This serves to point out why successful balances usually isolate the separate components.

In order to achieve the expected accuracy of the above results, a criterion of only one count variation in zero readings and damping difference could be established. This goal is easily reached with the damping circuits, since all acceptable runs had a zero variation over the test run time between heavily and lightly damped readings.

The problem of zero drift cannot be easily rectified with the existing system. Improvements were made to reduce the zero drift, such as installation of locks on all potentiometers and covers for all load cells to reduce thermal effects.

The existing power supply for the transducer-amplifier-driver units displayed variation in output voltage as high as 0.01 volts due to fluctuations in line voltage. This variation produced zero changes as high as twenty counts. In order to rectify this situation, a more stable 18.00 volt power supply should be implemented.

Investigation of circuit characteristics up to the balance design limits will require removal of the entire balance system to a more rigid location. A suitable load application method must be devised to accurately test the system to design limits.

## V. SYSTEM EVALUATION

It was established that the balance system performed fairly well under static calibration conditions. In order to evaluate the system under operating conditions, a calibration wing was tested in the 3.5 by 5.0 foot subsonic wind-tunnel.

The unswept, rectangular calibration wing incorporated a modified NACA 63-010 airfoil section, and had a constant 0.50 foot chord and 3.0 foot span (Figure 9). It was locally built from laminated mahogany glued to a 0.25 inch thick aluminum spar. The gray lacquer paint was hand rubbed to a smooth contour. The wing was mounted upon the two main strut supports and a tail-sting was attached to the movable tail-strut. The main struts were partially enclosed by two streamlined windshield fairings which were attached to the tunnel test section floor and presumably did not touch the struts. Figure 9 shows installation in the wind tunnel.

After obtaining static weight tares for an angle of attack range of -5.0 to +15.0 degrees (Table IV), the wing was subjected to a range of test-section dynamic pressures from 10.0 to 50.0 pounds per square foot.

The desired fast data acquisition characteristic proved extremely convenient. A typical traverse of -5.0 to +15.0 degrees angle of attack totalling twenty-five individual settings required an average of thirty minutes.

Extreme care must be taken to adjust all circuits as outlined in Appendix A. Of particular importance is the proper adjustment of the damping circuits to insure reliable results. At the completion of all runs, all zero settings and damping adjustments were checked. Any run that resulted in a deviation of output of more than two counts before and after damping application was rejected.

No aerodynamic strut tares were obtained at this time. As noted below, these tares may have been significant to the low drag and moment values existing.

All results obtained are presented in Table V, and are displayed in Figures 10, 11, and 12. Appendix B outlines all corrections applied during data reduction and presents a sample calculation. All data reduction was accomplished using a Wang Model 360 programmable calculator.

The lift results obtained were repeatable. All runs produced essentially the same lift coefficient versus angle of attack curve, as expected with the Reynolds number variations from 2.8 to 6.3 x $10^5$. The lift curve slope, $C_{L_\alpha}$, obtained was 0.0700 per degree.

In order to compare the value of $C_{L_\alpha}$ obtained for the rectangular wing, the theoretical value was calculated as outlined in Ref. 4:

$$C_{L_\alpha} = 2\pi k \frac{AR}{E\,AR + 2k\,(1 + \tau)}$$

where:

$$k = \frac{1 + \varepsilon}{1 + \varepsilon^2} \quad \text{with} \quad \varepsilon = \frac{4}{3\sqrt{3}} \times \text{airfoil thickness ratio}$$

$$E = \frac{\text{wing semi-perimeter}}{\text{wing span}}$$

$\tau$ = correction factor for deviation from elliptic loading

For the profile tested:

AR = 6.0 span = 3.0 ft. chord = 0.5 ft.

thickness ratio = 0.10

Therefore:

$$\varepsilon = \frac{4\ (.1)}{3\sqrt{3}} = 0.07698$$

$$k = \frac{1 + 0.07698}{1 + (0.07698)^2} = 1.0706$$

$$E = \frac{3.0 + 0.5}{3.0} = 1.6667$$

$\tau = 0.16545$ Ref. 4 p. 211

Therefore:

$$C_{L_\alpha} = \frac{(2)(\pi)(1.0706)(6.0)}{(1.6667)(6.0) + 2(1.0706)(1 + 0.16545)}$$

$$C_{L_\alpha} = 0.0742 \text{ per degree}$$

The experimental value of 0.0700 $deg^{-1}$ obtained for $C_{L_\alpha}$ compares favorably with the theoretical value of 0.0742 $deg^{-1}$. The $C_L$ vs. $\alpha$ curves show a maximum value of $C_L$ of approximately 0.72, which is not unreasonable considering that the airfoil sections were uncambered.

It will be noted from Figure 10 that the calibration wing has a zero lift angle of approximately +0.5 degrees. Several factors may contribute to this including tunnel flow inclination and aerodynamic tares due to support strut aerodynamic interference. A slight flow inclination of 0.25 degrees downwash was measured during flow calibrations in the tunnel in 1965, and this may partially account for about one-half of the discrepancy. Slight zero lift angle variations such as encountered here are not unusual, and they may be accounted for in a precise aerodynamic evaluation. The important thing to note is that they were consistent and repeatable.

The results obtained for pitching moment about the quarter chord, $C_{Mc/4}$, versus angle of attack and coefficient of drag, $C_D$, versus coefficient of lift were off by almost one order of magnitude when compared to a similar profile, NACA 63-009 [Ref. 1].

It is felt that this error is not solely attributable to balance measuring system inaccuracies. The expected value for $C_{Dmin}$, minimum coefficient of drag, were of the order of 0.0080 to 0.0100. At a dynamic pressure as high as 50.0 pounds per square foot, the three square foot area wing was expected to produce a drag force of only 1.2 pounds. The

magnitude of this reading may have been masked by the aerodynamic tares of the support system which were neglected in this determination. The magnitude of the moment may also have been masked by these tares.

There is a possibility that rubbing occurred between the windshields and the two main support struts. A clue to this is provided by the $C_{Mc/4}$ behavior at the higher dynamic pressures indicating a fairly well defined aerodynamic center near to the quarter chord while the behavior at the lower dynamic pressures was erratic. Also, the change in $C_{Dmin}$ with dynamic pressure suggests that the rubbing interference may have imposed an error in the horizontal loadings measured by the balance.

To correct these deficiencies, aerodynamic support tares must be accounted for or a redesign of the aerodynamic fairings accomplished. In addition, the installation of a grounding circuit to indicate fairing-support strut interference should be installed.

All circuits worked well in the evaluation of the system under operating conditions. The electronic damping circuits were adequate for drag and pitching moment measurements; however, at high angles of attack the onset of buffet caused considerable variation in readings due to the lack of mechanical damping. Some consideration should be given to the installation of a dashpot to provide mechanical damping of the lift linkage.

The model angle of attack rate under no-wind conditions has been measured as being 1.75 degrees per second. This rate is too high for precise adjustments in model attitude. Considerable time was spent attempting to set a specified model angle of attack, and an unskilled operator would have extreme difficulty. An improved Bodine shunt-wound D. C. motor has been received, and it is an adjustable rate system. Presumably, the installation of this new unit with a design variation in angle of attack

rate from 0.06 to 1.60 degrees per second should accommodate the desires of many varied operators.

A desirable characteristic of the balance system is the capability to generate lift curves, drag versus lift, etc., as the airfoil is rotated. This was not investigated at this time due to the high rotation rate of the pitch angle drive unit. This capability will be realized with the installation of the variable rate drive unit. Approximate drag and moment values can be taken from the summing circuits. For demonstration purposes, the accuracy of these outputs should be adequate.

The balance is presently mounted on an elastic floor structure, and hence is not firmly secured in an inertial reference frame. The sensitive load transducers are readily influenced by individuals walking nearby, and, at times, it is virtually impossible to make balance calibrations. Floor vibrations during tunnel operation also have an adverse influence. Plans are currently being made to isolate the balance platform to alleviate this problem. This improvement must be made before serious use of any wind-tunnel balance can be made with this wind-tunnel.

## VI. CONCLUSIONS AND RECOMMENDATIONS

The linearization of the load cell outputs of the electronic wind-tunnel balance has been accomplished. All transducer outputs are essentially linear over the designed load range.

In its present form, the balance is now suitable for student experiments in wind-tunnel techniques. The increased data acquisition rate and recording capability will be extremely valuable for the limited time available for student laboratory work such as in applied aerodynamics courses.

Some work must be undertaken to devise methods to obtain aerodynamic support tares for this system. An alternate solution would be a redesign and modification of the existing model support system to reduce the aerodynamic tares, such as a plate support used by some industrial wind-tunnels.

Installation of the variable rate pitch angle drive unit should be accomplished as soon as possible.

A study should be made as to the feasibility of the incorporation of a mechanical damper system into the lift linkage to damp out oscillations at high angles of attack. Additionally, it should be possible to make check calibrations of the balance while a model is installed in order to authenticate the operation of the balance readout system. The lift load cell has this feature already, since a dead weight can be placed on the support cross tube even when a model is present. Similar arrangements should be designed for spot checking the remaining two constraint link calibrations.

Current plans for the isolation of the balance platform from the wind-tunnel support frame should be completed and implemented. This change is mandatory before serious model test work can take place.

TABLE I

Lift Calibration

| Load | Lift | Load | Lift | Load | Lift | Load | Lift | Load | Lift | Load | Lift |
|---|---|---|---|---|---|---|---|---|---|---|---|
| 0.0 | 0.0 | 52.0 | 52.1 | 104.0 | 104.0 | 0.0 | 0.0 | -52.0 | -52.4 | -104.0 | -104.3 |
| 2.0 | 2.0 | 54.0 | 54.1 | 106.0 | 106.0 | -2.0 | -2.0 | -54.0 | -54.4 | -106.0 | -106.3 |
| 4.0 | 4.0 | 56.0 | 56.0 | 108.0 | 108.0 | -4.0 | -4.1 | -56.0 | -56.4 | -108.0 | -108.4 |
| 6.0 | 6.0 | 58.0 | 58.1 | 110.0 | 110.0 | -6.0 | -6.0 | -58.0 | -58.5 | -110.0 | -110.3 |
| 8.0 | 8.0 | 60.0 | 60.1 | 112.0 | 112.0 | -8.0 | -8.0 | -60.0 | -60.5 | -112.0 | -112.3 |
| 10.0 | 10.0 | 62.0 | 62.1 | 114.0 | 113.9 | -10.0 | -10.1 | -62.0 | -62.4 | -114.0 | -114.2 |
| 12.0 | 12.0 | 64.0 | 64.0 | 116.0 | 115.9 | -12.0 | -12.0 | -64.0 | -64.4 | -116.0 | -116.2 |
| 14.0 | 14.0 | 66.0 | 66.1 | 118.0 | 117.9 | -14.0 | -14.0 | -66.0 | -66.4 | -118.0 | -118.1 |
| 16.0 | 16.0 | 68.0 | 68.0 | 120.0 | 119.9 | -16.0 | -16.0 | -68.0 | -68.4 | -120.0 | -120.2 |
| 18.0 | 18.0 | 70.0 | 70.1 | 122.0 | 121.9 | -18.0 | -18.1 | -70.0 | -70.4 | -122.0 | -122.2 |
| 20.0 | 20.1 | 72.0 | 72.1 | 124.0 | 124.0 | -20.0 | -20.0 | -72.0 | -72.4 | -124.0 | -124.2 |
| 22.0 | 22.1 | 74.0 | 74.1 | 126.0 | 126.1 | -22.0 | -22.0 | -74.0 | -74.4 | -126.0 | -126.2 |
| 24.0 | 24.0 | 76.0 | 76.0 | 128.0 | 128.0 | -24.0 | -24.1 | -76.0 | -76.4 | -128.0 | -128.1 |
| 26.0 | 26.0 | 78.0 | 78.1 | 130.0 | 130.0 | -26.0 | -26.0 | -78.0 | -78.4 | -130.0 | -130.1 |
| 28.0 | 28.0 | 80.0 | 80.1 | 132.0 | 132.0 | -28.0 | -28.4 | -80.0 | -80.4 | -132.0 | -132.1 |
| 30.0 | 30.0 | 82.0 | 82.1 | 134.0 | 134.0 | -30.0 | -30.4 | -82.0 | -82.4 | -134.0 | -134.1 |
| 32.0 | 32.0 | 84.0 | 84.0 | 136.0 | 136.0 | -32.0 | -32.4 | -84.0 | -84.4 | -136.0 | -136.1 |
| 34.0 | 34.0 | 86.0 | 86.0 | 138.0 | 138.0 | -34.0 | -34.4 | -86.0 | -86.4 | -138.0 | -138.1 |
| 36.0 | 36.1 | 88.0 | 88.0 | 140.0 | 140.0 | -36.0 | -36.4 | -88.0 | -88.4 | -140.0 | -140.0 |
| 38.0 | 38.1 | 90.0 | 90.1 | 142.0 | 142.0 | -38.0 | -38.4 | -90.0 | -90.3 | -142.0 | -142.0 |
| 40.0 | 40.1 | 92.0 | 92.1 | 144.0 | 144.0 | -40.0 | -40.4 | -92.0 | -92.3 | -144.0 | -144.0 |
| 42.0 | 42.1 | 94.0 | 94.0 | 146.0 | 146.0 | -42.0 | -42.3 | -94.0 | -94.3 | -146.0 | -146.0 |
| 44.0 | 44.1 | 96.0 | 96.0 | 148.0 | 148.0 | -44.0 | -44.3 | -96.0 | -96.3 | -148.0 | -148.0 |
| 46.0 | 46.1 | 98.0 | 98.0 | 150.0 | 150.0 | -46.0 | -46.3 | -98.0 | -98.3 | -150.0 | -150.0 |
| 48.0 | 48.1 | 100.0 | 100.1 | 152.0 | 152.0 | -48.0 | -48.2 | -100.0 | -100.3 | -152.0 | -152.0 |
| 50.0 | 50.1 | 102.0 | 102.1 | 154.0 | 154.0 | -50.0 | -50.3 | -102.0 | -102.4 | -154.0 | -154.0 |

TABLE II

Drag-Moment Calibration

| DRAG (pounds) | | MOMENT (inch pounds) | | MOMENT (inch pounds) | |
|---|---|---|---|---|---|
| Load | Reading | Load | Reading | Load | Reading |
| 0.0 | 0.00 | 0.0 | 0.00 | 0.0 | 0.00 |
| 2.0 | 1.90 | 20.0 | 19.72 | -20.0 | -19.72 |
| 4.0 | 3.91 | 40.0 | 39.60 | -40.0 | -39.45 |
| 6.0 | 5.90 | 60.0 | 59.47 | -60.0 | -59.17 |
| 8.0 | 7.93 | 80.0 | 79.35 | -80.0 | -79.05 |
| 10.0 | 9.94 | 100.0 | 101.99 | -100.0 | -99.08 |
| 12.0 | 11.90 | 120.0 | 120.37 | -120.0 | -120.80 |
| 14.0 | 13.89 | 140.0 | 140.74 | -140.0 | -140.67 |
| 16.0 | 15.87 | 160.0 | 161.11 | -160.0 | -160.54 |
| 18.0 | 17.88 | 180.0 | 181.80 | -180.0 | -180.27 |
| 20.0 | 19.94 | 200.0 | 200.00 | -200.0 | -200.14 |
| 22.0 | 21.96 | 220.0 | 222.36 | -220.0 | -220.01 |
| 24.0 | 23.97 | 240.0 | 240.74 | -240.0 | -239.89 |
| 26.0 | 25.91 | 260.0 | 261.25 | -260.0 | -259.76 |
| 28.0 | 27.98 | 280.0 | 279.63 | -280.0 | -279.78 |
| 30.0 | 29.98 | 300.0 | 300.00 | -300.0 | -299.66 |
| 32.0 | 32.01 | 320.0 | 320.13 | -320.0 | -319.28 |
| 34.0 | 34.08 | 340.0 | 340.88 | -340.0 | -339.26 |
| 36.0 | 36.05 | 360.0 | 361.25 | -360.0 | -359.13 |
| 38.0 | 38.05 | 380.0 | 381.62 | -380.0 | -381.15 |
| 40.0 | 40.02 | 400.0 | 402.13 | -400.0 | -401.03 |
| 42.0 | 42.09 | 420.0 | 418.52 | -420.0 | -420.90 |
| 44.0 | 44.05 | 440.0 | 438.89 | -440.0 | -442.78 |
| 46.0 | 46.05 | 460.0 | 459.26 | -460.0 | -460.50 |
| 48.0 | 48.16 | 480.0 | 477.64 | -480.0 | -482.52 |
| 50.0 | 50.19 | 500.0 | 500.14 | -500.0 | -502.54 |

TABLE III

Drag-Moment Calibration Confirmation

| LOADING CONDITION | | RESULTS | | LOADING CONDITION | | RESULTS | |
|---|---|---|---|---|---|---|---|
| Drag (lb) | Moment (in lb) | Drag (lb) | Moment (in lb) | Drag (lb) | Moment (in lb) | Drag (lb) | Moment (in lb) |
| 25.00 | -40.00 | 24.90 | -40.60 | 10.00 | -100.00 | 9.88 | -99.22 |
| 25.00 | -80.00 | 24.86 | -80.34 | 20.00 | -100.00 | 19.82 | -99.23 |
| 25.00 | -120.00 | 24.89 | -119.79 | 30.00 | -100.00 | 29.96 | -100.77 |
| 25.00 | -160.00 | 24.88 | -159.39 | 35.00 | -100.00 | 34.85 | -99.92 |
| 25.00 | -200.00 | 24.92 | -201.29 | 40.00 | -100.00 | 39.90 | -100.77 |
| 25.00 | -240.00 | 24.92 | -240.89 | 45.00 | -100.00 | 44.88 | -99.47 |
| 25.00 | -280.00 | 24.92 | -280.49 | 50.00 | -100.00 | 49.90 | -100.47 |
| 25.00 | -320.00 | 24.94 | -319.94 | | | | |
| 25.00 | -360.00 | 24.91 | -359.68 | | | | |
| 25.00 | -400.00 | 24.91 | -399.28 | | | | |
| 25.00 | -440.00 | 24.87 | -439.03 | | | | |

TABLE IV

Static Weight Tares

| Angle of Attack | Load Cell 1 (mv) | Load Cell 2 (mv) | Load Cell 3 (mv) |
|---|---|---|---|
| -5.01 | 0 | 0 | 0 |
| -4.00 | 0 | 0 | 0 |
| -2.99 | 0 | 0 | 0 |
| -2.00 | 0 | 0 | 0 |
| -1.01 | 0 | 0 | 0 |
| 0.00 | 0 | 0 | 0 |
| 1.02 | 0 | 0 | 0 |
| 2.00 | 0 | 0 | 0 |
| 3.01 | 0 | 0 | 0 |
| 4.03 | 0 | 0 | 0 |
| 5.01 | 0 | 0 | 0 |
| 6.03 | 0 | 0 | 0 |
| 7.02 | 0 | 0 | 0 |
| 8.02 | 0 | .1 | -0 |
| 9.01 | 0 | 1 | -0 |
| 9.99 | 0 | 2 | -0 |
| 11.02 | 0 | 3 | -0 |
| 12.01 | 0 | 3 | -0 |
| 13.02 | 0 | 3 | -0 |
| 13.99 | 0 | 4 | -0 |
| 15.02 | 0 | 5 | -1 |

TABLE Va

NPS Calibration Wing Results

. Run 12

q = 10.0 psf

| $\alpha$ | $C_L$ | $C_D$ | $C_{M_{c/4}}$ |
|---|---|---|---|
| -5.34 | -.464 | .0316 | .0231 |
| -4.29 | -.378 | .0269 | .0198 |
| -3.20 | -.285 | .0196 | .0420 |
| -2.14 | -.219 | .0172 | .0404 |
| -0.02 | -.020 | .0140 | .0388 |
| 1.04 | +.033 | .0167 | .0132 |
| 2.05 | .106 | .0121 | .0371 |
| 3.11 | .172 | .0103 | .0627 |
| 4.18 | .291 | .0149 | .0388 |
| 5.23 | .331 | .0199 | .0420 |
| 6.26 | .398 | .0197 | .0692 |
| 7.29 | .450 | .0242 | .0726 |
| 8.37 | .510 | .0381 | .0552 |
| 9.41 | .584 | .0497 | .0636 |
| 10.45 | .610 | .0548 | .1500 |
| 11.49 | .696 | .0900 | .1220 |
| 12.07 | .796 | .1069 | .1064 |
| 12.50 | .729 | .1211 | .0636 |
| 12.99 | .703 | .1354 | .0751 |
| 13.50 | .696 | .1506 | .0323 |
| 13.96 | .676 | .1590 | .0389 |
| 14.47 | .649 | .1599 | .0950 |
| 14.98 | .643 | .1685 | .1056 |
| 15.43 | .624 | .1790 | .0554 |

TABLE Vb

NPS Calibration Wing Results

Run 21

q = 20.0 psf

| $\alpha$ | $C_L$ | $C_D$ | $C_{M_{c/4}}$ |
|---|---|---|---|
| -5.31 | -.431 | .0303 | .0087 |
| -4.26 | -.368 | .0245 | .0182 |
| -3.21 | -.295 | .0209 | .0157 |
| -2.16 | -.219 | .0183 | .0141 |
| -1.09 | -.132 | .0170 | .0132 |
| -0.03 | -.047 | .0145 | .0252 |
| 1.04 | .033 | .0145 | .0252 |
| 2.05 | .090 | .0156 | .0260 |
| 3.12 | .172 | .0146 | .0387 |
| 4.18 | .246 | .0158 | .0532 |
| 5.26 | .328 | .0184 | .0548 |
| 6.25 | .391 | .0221 | .0573 |
| 7.32 | .457 | .0256 | .0733 |
| 8.35 | .527 | .0326 | .0783 |
| 9.44 | .607 | .0462 | .0882 |
| 10.46 | .663 | .0646 | .1158 |
| 11.50 | .696 | .0949 | .0981 |
| 12.01 | .709 | .1046 | .1056 |
| 12.49 | .709 | .1151 | .1138 |
| 12.99 | .713 | .1279 | .1102 |
| 13.49 | .699 | .1395 | .0921 |
| 14.00 | .719 | .1514 | .1011 |
| 14.48 | .703 | .1595 | .1077 |
| 14.99 | .693 | .1680 | .1007 |
| 15.50 | .683 | .1784 | .0954 |

TABLE Vd

NPS Calibration Wing Results

Run 40

$\bar{q}$ = 40.0 psf

| $\alpha$ | $C_L$ | $C_D$ | $C_{M_{c/4}}$ |
|---|---|---|---|
| -5.28 | -.400 | .0399 | -.0387 |
| -4.23 | -.328 | .0345 | -.0356 |
| -3.19 | -.256 | .0314 | -.0377 |
| -2.13 | -.187 | .0291 | -.0393 |
| -1.08 | -.109 | .0276 | -.0401 |
| -0.03 | -.040 | .0270 | -.0406 |
| 1.02 | .035 | .0270 | -.0406 |
| 2.09 | .111 | .0276 | -.0401 |
| 3.13 | .182 | .0301 | -.0453 |
| 4.18 | .254 | .0314 | -.0377 |
| 5.22 | .328 | .0350 | -.0352 |
| 6.30 | .395 | .0375 | -.0267 |
| 7.34 | .479 | .0425 | -.0234 |
| 8.40 | .549 | .0503 | -.0249 |
| 9.44 | .610 | .0626 | -.0158 |
| 10.47 | .654 | .0789 | -.0102 |
| 11.51 | .699 | .1051 | -.0176 |
| 11.98 | .701 | .1174 | -.0217 |
| 12.49 | .708 | .1303 | -.0322 |
| 13.01 | .713 | .1444 | -.0486 |
| 13.49 | .716 | .1549 | -.0472 |
| 14.00 | .718 | .1666 | -.0517 |
| 14.50 | .698 | .1751 | -.0462 |
| 15.01 | .704 | .1727 | -.0468 |
| 15.51 | .686 | .1827 | -.0525 |

TABLE Vc

NPS Calibration Wing Results

Run 31

q = 30.0 psf

| $\alpha$ | $C_L$ | $C_D$ | $C_{M_{c/4}}$ |
|---|---|---|---|
| -5.30 | -.416 | .0335 | .0157 |
| -4.23 | -.338 | .0286 | .0124 |
| -3.17 | -.257 | .0245 | .0096 |
| -2.12 | -.183 | .0237 | .0000 |
| -1.09 | -.112 | .0212 | .0074 |
| -0.02 | -.027 | .0218 | .0011 |
| 1.03 | .042 | .0211 | .0074 |
| 2.08 | .115 | .0212 | .0074 |
| 3.15 | .199 | .0228 | .0086 |
| 4.19 | .268 | .0250 | .0181 |
| 5.23 | .338 | .0264 | .0198 |
| 6.30 | .414 | .0306 | .0226 |
| 7.33 | .486 | .0353 | .0259 |
| 8.43 | .546 | .0422 | .0399 |
| 9.42 | .595 | .0528 | .0385 |
| 10.45 | .647 | .0693 | .0602 |
| 11.47 | .685 | .0947 | .0523 |
| 12.01 | .694 | .1086 | .0356 |
| 12.49 | .707 | .1199 | .0353 |
| 13.00 | .712 | .1319 | .0356 |
| 13.53 | .720 | .1466 | .0194 |
| 14.00 | .709 | .1562 | .0271 |
| 14.53 | .723 | .1666 | .0444 |
| 14.98 | .707 | .1766 | .0249 |
| 15.52 | .696 | .1877 | .0156 |

TABLE Ve

NPS Calibration Wing Results

Run 50

q = 50.0 psf

| $\alpha$ | $C_L$ | $C_D$ | $C_{M_{c/4}}$ |
|---|---|---|---|
| -5.27 | -.398 | .0400 | -.0413 |
| -4.22 | -.330 | .0356 | -.0388 |
| -3.15 | -.262 | .0316 | -.0360 |
| -2.13 | -.190 | .0307 | -.0422 |
| -1.09 | -.110 | .0290 | -.0431 |
| 0.00 | -.031 | .0280 | -.0384 |
| 1.06 | .044 | .0263 | -.0288 |
| 2.10 | .119 | .0276 | -.0332 |
| 3.14 | .195 | .0301 | -.0370 |
| 4.22 | .266 | .0327 | -.0354 |
| 5.25 | .339 | .0357 | -.0334 |
| 6.29 | .409 | .0409 | -.0406 |
| 7.33 | .482 | .0449 | -.0326 |
| 8.40 | .561 | .0521 | -.0331 |
| 9.45 | .625 | .0652 | -.0289 |
| 10.48 | .673 | .0853 | -.0192 |
| 11.49 | .707 | .1127 | -.0310 |
| 12.00 | .713 | .1287 | -.0514 |
| 12.51 | .724 | .1416 | -.0524 |
| 13.02 | .723 | .1534 | -.0595 |
| 13.49 | .709 | .1652 | -.0720 |
| 13.98 | .704 | .1759 | -.0855 |
| 14.50 | .699 | .1826 | -.0527 |
| 14.97 | .673 | .1927 | -.0882 |
| 15.48 | .675 | .2018 | -.0868 |

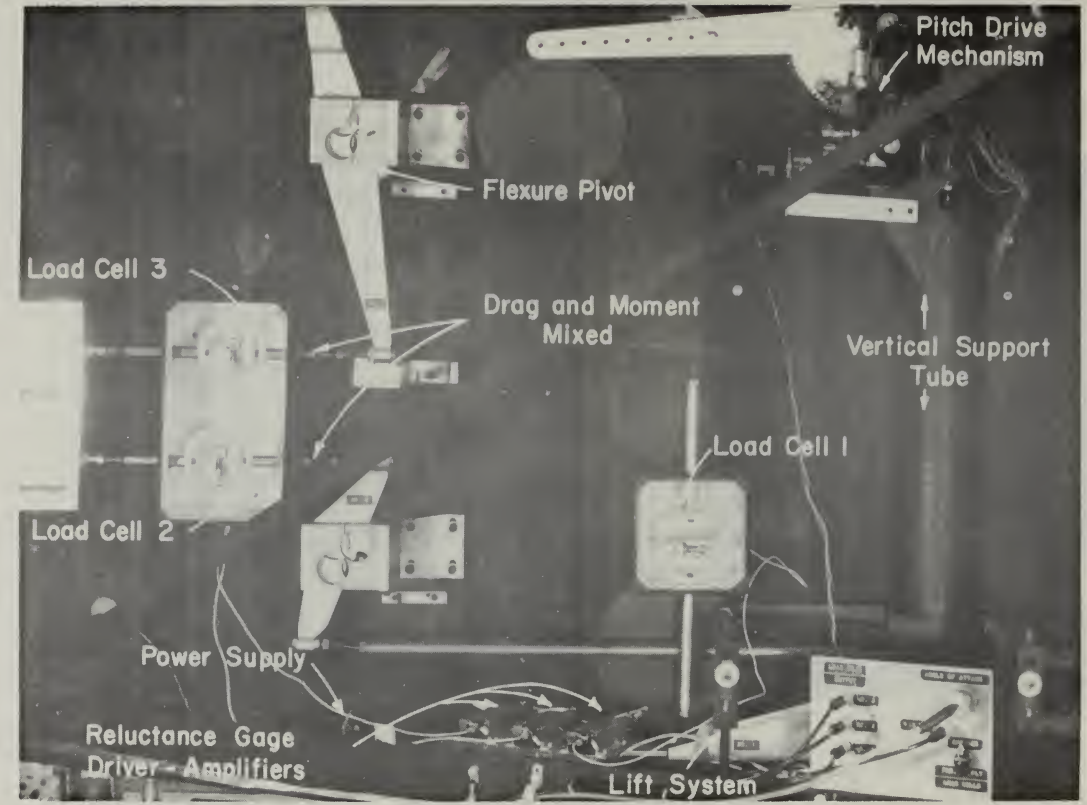


Figure 1. Electronic Wind-Tunnel Balance

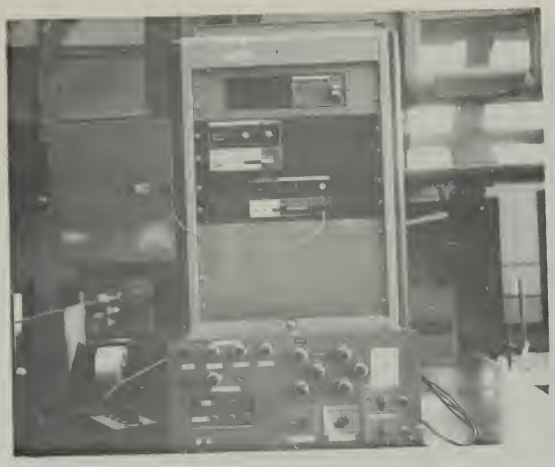

a. Remote Control Station


b. Control Panel

Figure 2. System Components

a. Micrometer Calibration Device

b. Calibration Frame in Tunnel

Figure 3. Calibration Equipment

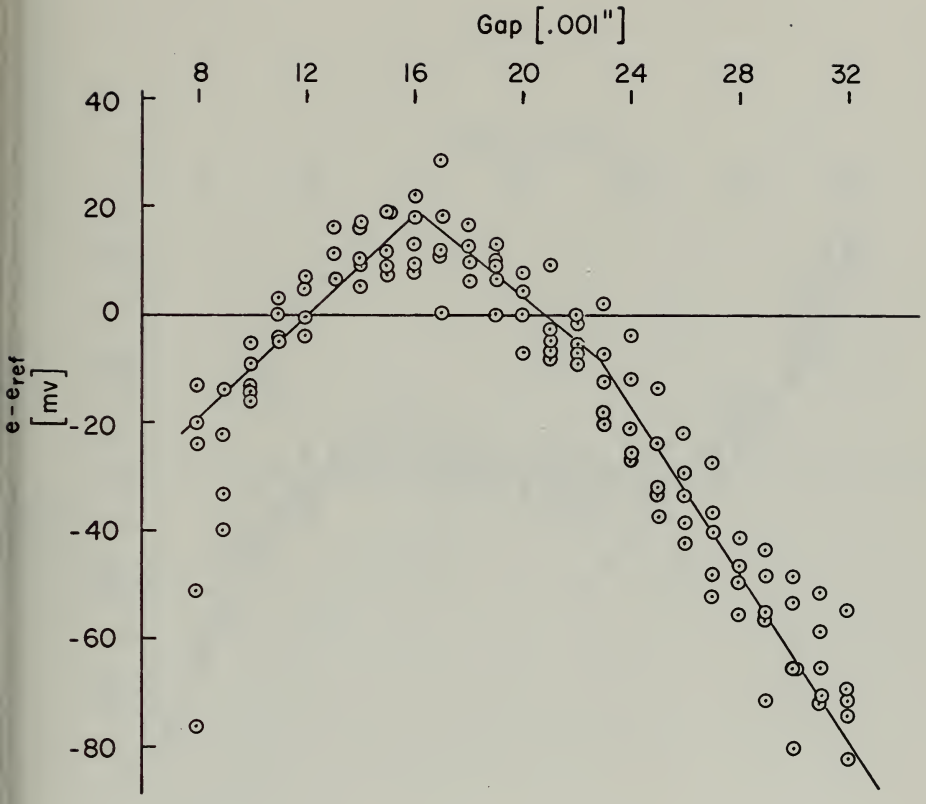


FIGURE 4. LOAD CELL ONE OUTPUT

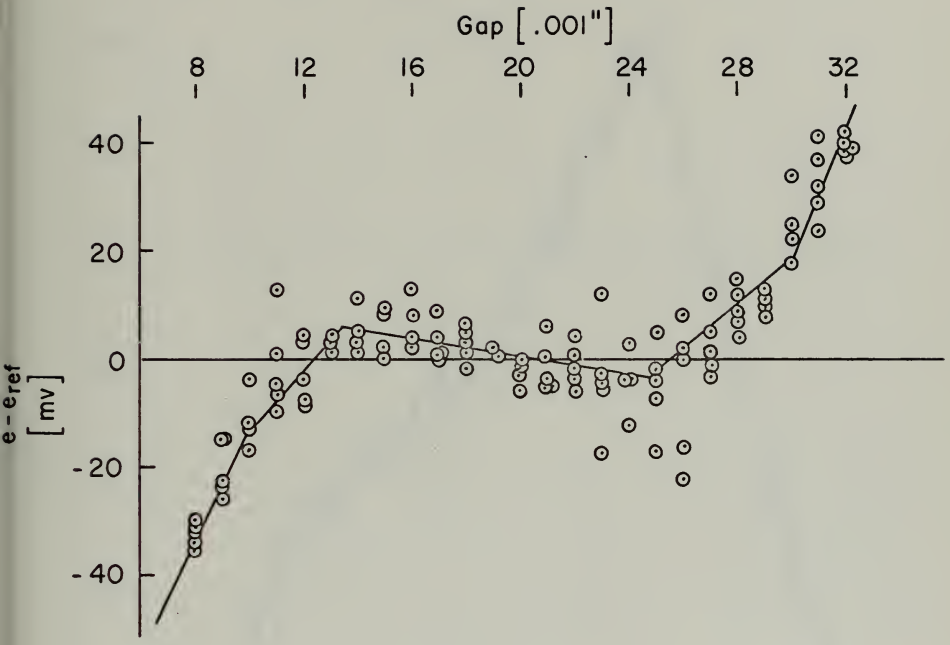


FIGURE 5. LOAD CELL TWO OUTPUT

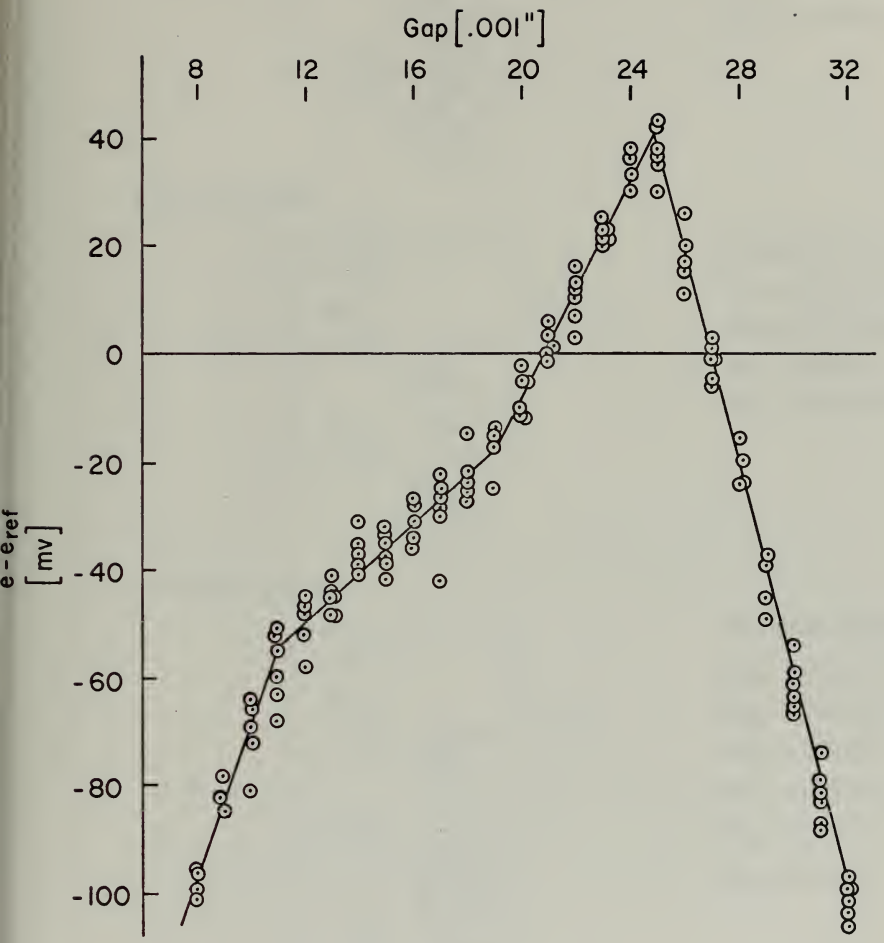


FIGURE 6. LOAD CELL THREE OUTPUT

Load Cell One

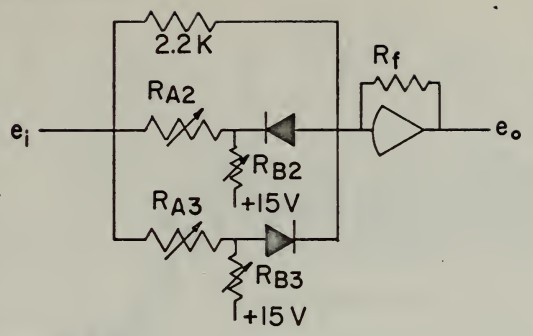


Nominal Values

$R_{A2}$ = 27.8 K
$R_{B2}$ = 143.0K
$R_{A3}$ = 37.6 K
$R_{B3}$ = 115.9 K

Load Cell Two

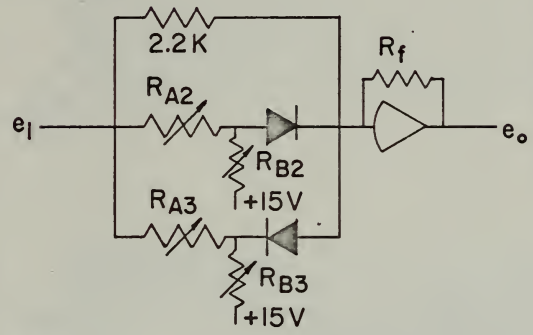


Nominal Values

$R_{A2}$ = 93.4 K
$R_{B2}$ = 403.0 K
$R_{A3}$ = 89.5 K
$R_{B3}$ = 190.0 K

Load Cell Three

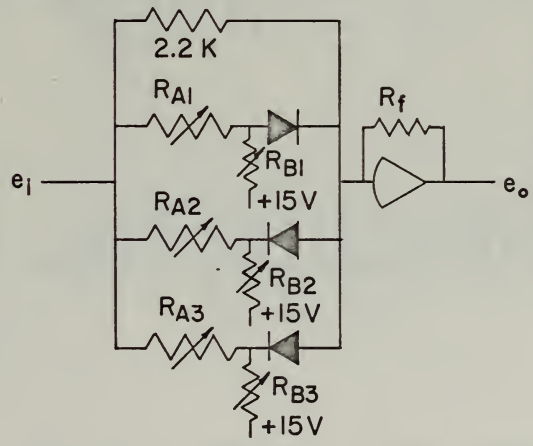


Nominal Values

$R_{A1}$ = 55.6 K
$R_{B1}$ = 230.0 K
$R_{A2}$ = 63.8 K
$R_{B2}$ = 138.2 K
$R_{A3}$ = 31.2 K
$R_{B3}$ = 61.1 K

FIGURE 7. LOAD CELL LINEARIZATION CIRCUITS

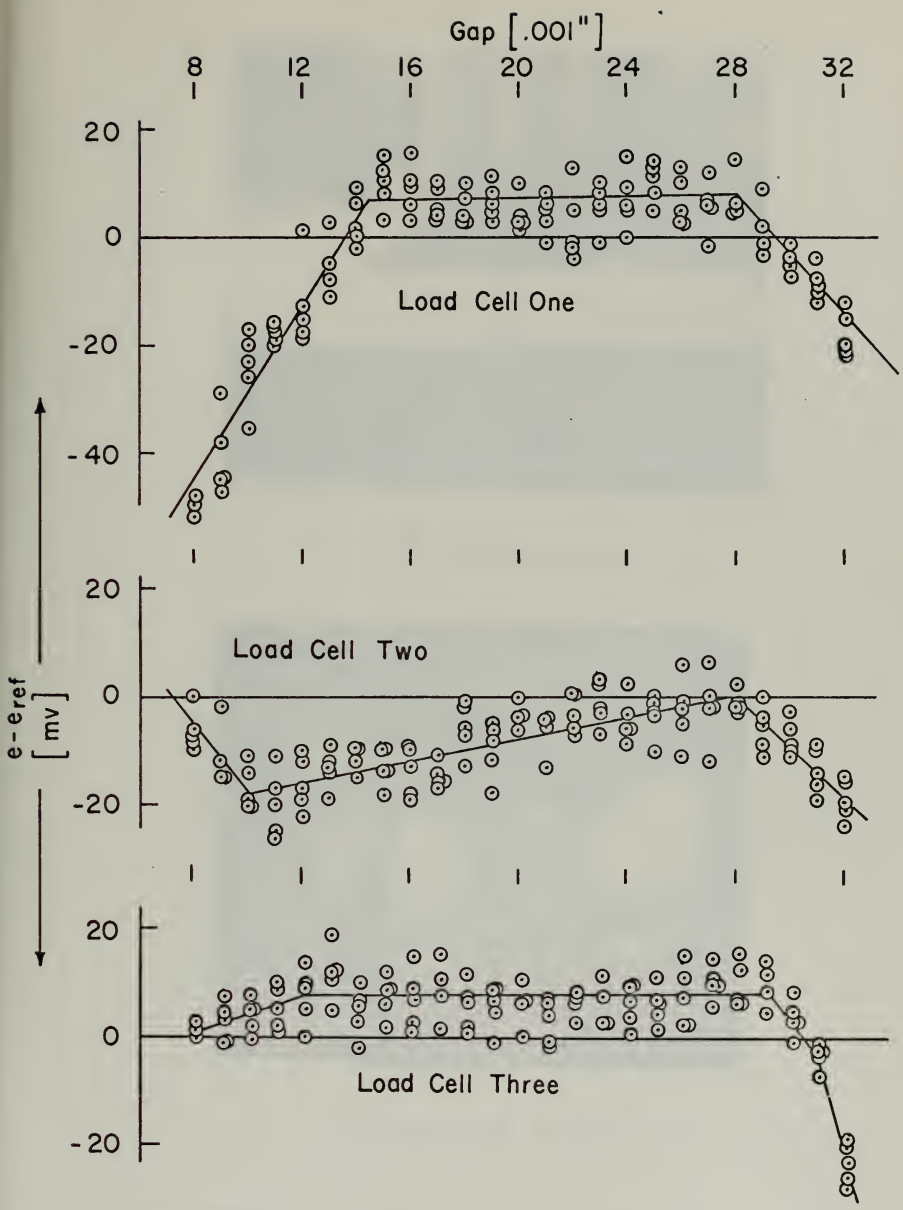


FIGURE 8. LOAD CELL OUTPUT AFTER LINEARIZATION

a. NPS Calibration Wing

b. Wing Installed in Tunnel

Figure 9. Calibration Wing

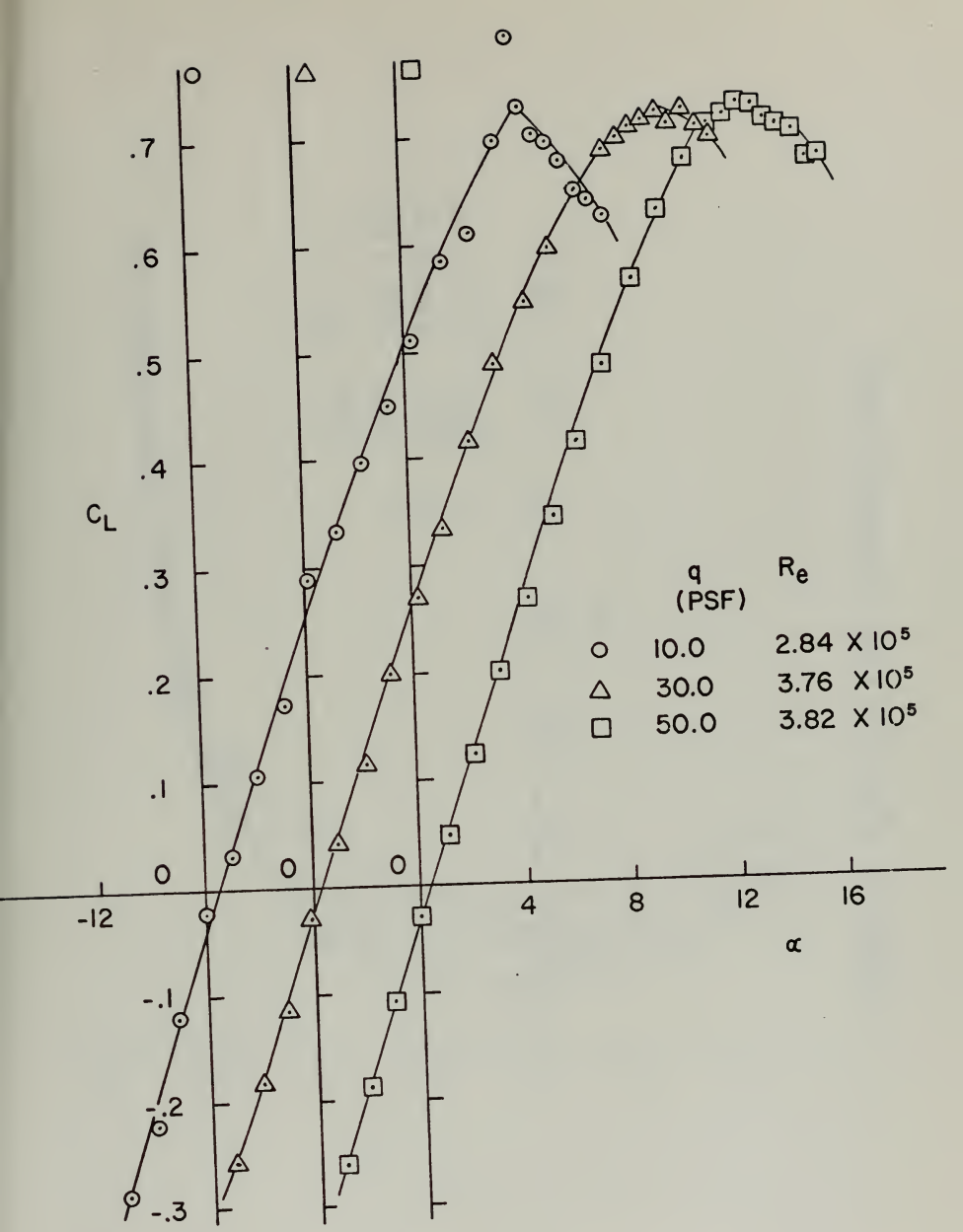


FIGURE 10. $C_L$ VS. α , NPS CALIBRATION WING

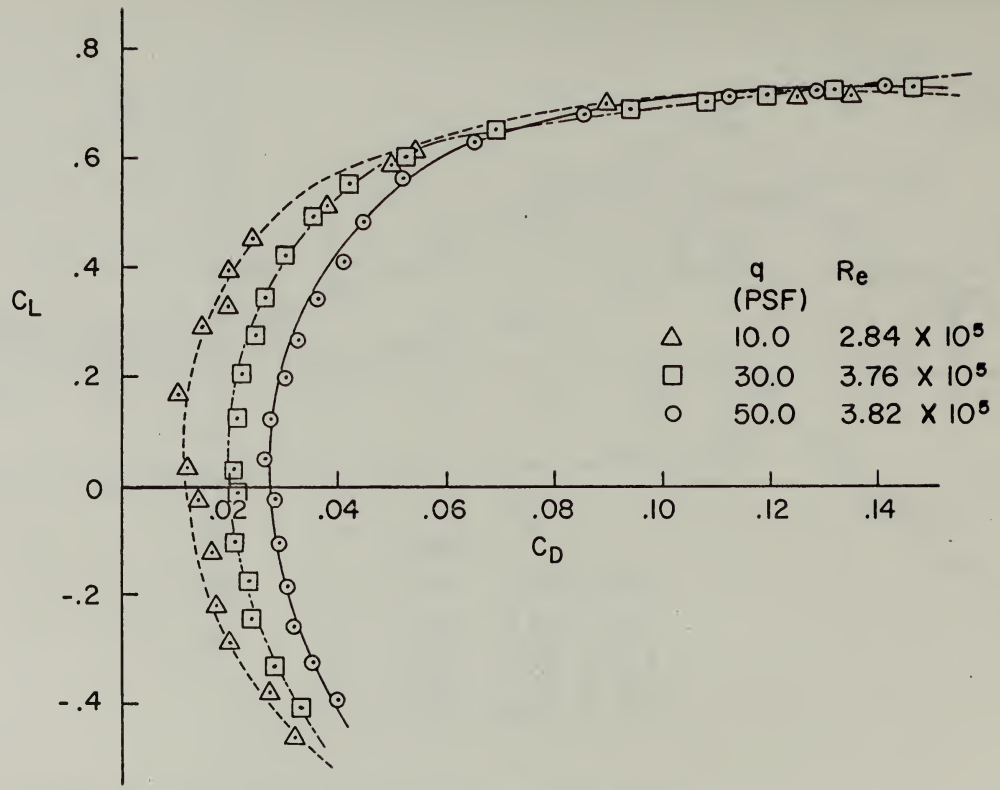


FIGURE 11. $C_L$ VS. $C_D$, NPS CALIBRATION WING

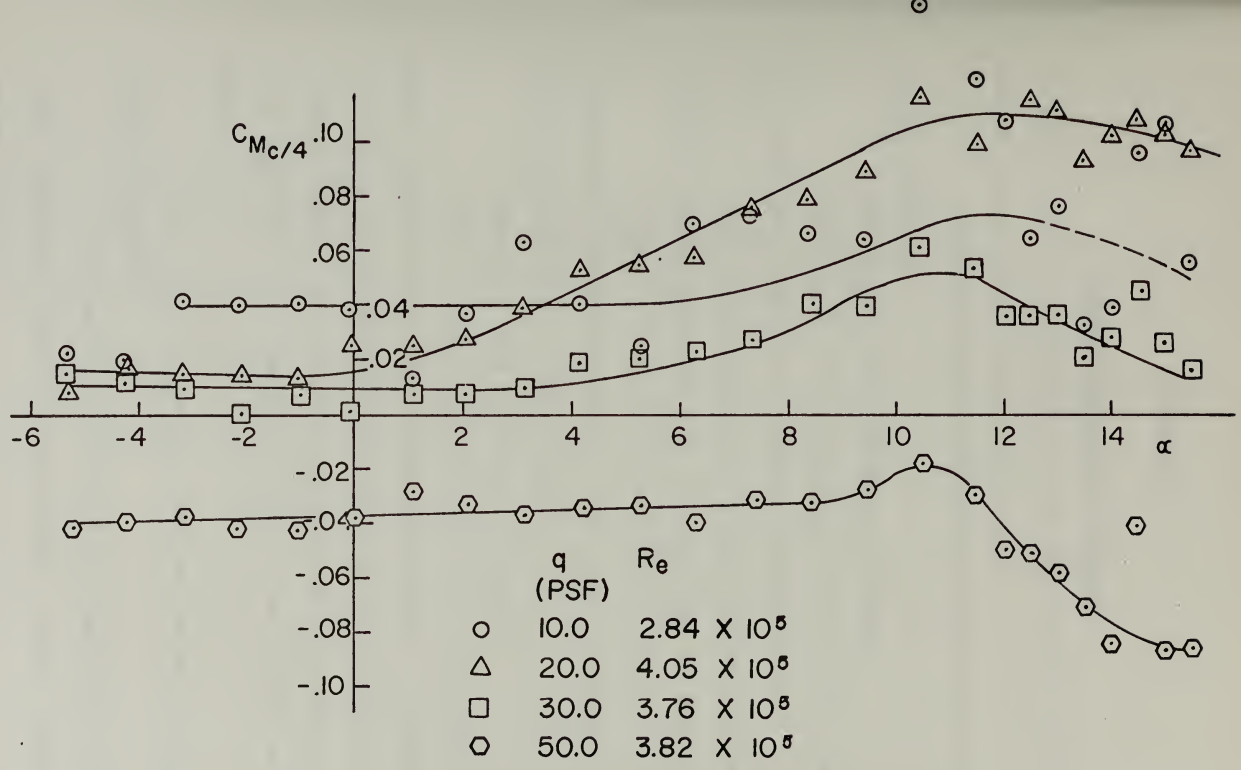


FIGURE 12. $C_{M_{c/4}}$ VS. α , NPS CALIBRATION WING

## APPENDIX A

### EQUIPMENT ADJUSTMENT PROCEDURES

In order to insure optimum results using the electronic balance system, the following procedures must be adhered to:

1. Allow a minimum of thirty minutes warm-up time for all system components.

2. Adjust zero and calibration of voltmeter.

3. Check, and adjust if necessary, the proximeter power supply at 18.00 volts. (Position 9 on variable output switch).

4. With all damping at zero, adjust all load cell readings to zero (with output setting on lift, load cells two and three damped).

5. Adjust "offset adjust" potentiometers for all load cells until there is no variation between light and heavy damping. This is a critical step to insure reliable results.

6. Reset all load cell zeros as required.

7. Adjust model to zero reference angle using bubble level on model levelling plugs on wing calibration template. The vernier scale at the rear of the balance may be used to check calibrations of angular changes, however, the electrical output of the angle indication system must be nulled to read zero when the model is at its zero reference position.

8. Just prior to starting a data run, recheck all zeros and damping adjustments.

9. At the completion of every run, recheck zeros and damping offset adjustments. Deviations of more than two counts seriously derogate results.

## APPENDIX B

### DATA REDUCTION

The raw data yields lift directly in pounds, angle of attack in degrees, and drag and moment mixed as outputs of load cells two and three ($e_{2u}$ and $e_{3u}$).

Apply the static weight tare corrections, $\Delta e_2$ and $\Delta e_3$, to load cells two and three readings as needed:

$$e_2 = e_{2u} - \Delta e_2$$

$$e_3 = e_{3u} - \Delta e_3$$

Subsequently, since balance calibration was:

$$-27.666\ D - 0.8818\ M = e_2 \text{ (mv)}$$

$$29.578\ D + 0.4776\ M = e_3 \text{ (mv)}$$

Then we may consider:

$$\begin{bmatrix} -27.666 & -.8818 \\ 29.578 & .4776 \end{bmatrix} \begin{Bmatrix} D \\ M \end{Bmatrix} = \begin{Bmatrix} e_2 \\ e_3 \end{Bmatrix}$$

or:

$$\begin{Bmatrix} D \\ M \end{Bmatrix} = \begin{bmatrix} .03714 & .06855 \\ -2.2996 & -2.1508 \end{bmatrix} \begin{Bmatrix} e_2 \\ e_3 \end{Bmatrix}$$

yielding drag in pounds and moment in inch pounds.

Calculate:

$$C_{Lu} = \frac{L}{q\,S}$$

$$C_{Du} = \frac{D}{q\,S}$$

$$C_{Mc/4u} = \frac{M}{q\,S\,\bar{c}}$$

where consistent units are used.

The angle of attack and aerodynamic coefficients obtained above must be then corrected for wind-tunnel boundary effects. Because of the model's small size, no blocking corrections were necessary. Spanwise variations in angle of attack were ignored as the wing span of the model was less than 0.8 of the tunnel width.

Total change in angle of attack, $\Delta\alpha_A$ :

$$\Delta\alpha_A = \Delta\alpha + \tau_2\Delta\alpha = (1 + \tau_2)\Delta\alpha$$

where

$$\Delta\alpha = \frac{S}{C} C_{Lu}\delta = \text{correction for constant downwash}$$

$\tau_2$ = correction for variation of downwash with chord

$\delta$ = boundary correction factor

$C$ = wind-tunnel cross-sectional area

The lift coefficient, $C_{L_u}$, must be corrected for the fact that the chordwise variation of downwash has changed the apparent camber of the airfoil. The change in lift coefficient, $\Delta C_L$:

$$C_L = |\Delta\alpha| a \quad \text{(subtracted from } C_L\text{)}$$

where: $a$ = measured lift curve slope, $C_{L_\alpha}$ .

The change in drag coefficient due to an alteration in downwash is:

$$\Delta C_D = |\Delta\alpha| C_L \quad \text{(added to } C_{D_u}\text{)}.$$

The change in lift due to change in apparent camber will also cause a change in pitching moment about the quarter chord; however, the magnitude of this change, 0.25 ( $\Delta C_L$) is small and will be neglected. Thus:

$$C_{m_{c/4u}} = C_{m_{c/4}}$$

The following dimensions of the calibration wing were utilized in all calculations;

Span, = 3.0 ft.

Chord, c = 0.5 ft. = constant

Taper ratio, $\lambda_T = 1.0$

Aspect Ratio, AR = 6.0

Area, S = 1.5 ft.$^2$

All wind-tunnel correction factors applied were obtained from Ref. 5. Suitable correction factors were not available for the elongated octagonal test section of the 3.5 by 5.0 foot subsonic wind-tunnel. In order to obtain correction factors, the best fitting ellipse to approximate the test section was obtained from scale drawings. The major axis, B, of the resulting ellipse was 5.125 feet and the minor axis, h, was 3.625 feet. The ratio of the minor axis to the major axis, $\lambda$ , was 0.707. The test section cross-sectional area, C, was 14.48 square feet.

To obtain the downwash correction factor, $\tau_2$:

From Ref. 5, Figure 6:53:

with

$$\frac{\text{Tail length}}{\text{tunnel width}} = \frac{c/4}{B} = \frac{0.125}{5.125} = 0.0244$$

$\tau_2 = 0.12$ for the closed elliptic jet

To obtain the boundary correction factor, $\delta$ :

From Ref. 5, Figure 6:23:

$\frac{b_v}{b} = 0.87$ with $\lambda_T = 1.0$ and AR = 6.0

Therefore effective span, $b_e$:

$$b_e = \frac{b}{2}\left(1 + \frac{b_v}{b}\right) = 0.935\ b$$

$b_e = 2.81$ feet

From Ref. 5, Figure 6:41:

$\delta = 0.105$

with

$$\frac{\text{Effective span}}{\text{Jet width}} = k = \frac{2.81}{5.125} = 0.548$$

$$\lambda = \frac{h}{B} = 0.707$$

SAMPLE CALCULATION:

For run 31, dynamic pressure, q = 30.0 pounds per square foot:

$\alpha_u$ = 4.00 degrees

L = 12.1 pounds

$e_{2_u}$ = -33 millivolts

$e_{3_u}$ = 33 millivolts

$\Delta e_2$ = 0

$\Delta e_3$ = 0

Therefore:

$$e_2 = e_{2_u} - \Delta e_2 = -33 \text{ mv.}$$
$$e_3 = e_{3_u} - \Delta e_3 = 33 \text{ mv}$$

Hence:

D = 1.09 pounds

M = 4.90 pounds

Aerodynamic coefficients:

$$C_{L_u} = \frac{12.1}{(30)(1.5)} = 0.269$$

$$C_{D_u} = \frac{1.09}{(30)(1.5)} = 0.0242$$

$$C_{M_{c/4u}} = C_{M_{c/4}} = \frac{4.90}{(30)(1.5)(6.0)} = 0.0181$$

Plotting $C_{L_u}$ vs. $\alpha_u$ yields:

a = 4.24 per radian

With wind-tunnel correction:

$$\alpha = 4.00 + (1 + 0.12)\frac{(1.50)}{(14.48)}(0.269)(.105)\frac{(180)}{\pi}$$

$$" = 4.19 \text{ degrees}$$

$$C_L = 0.269 - (0.12)\frac{(1.50)}{(14.48)}(0.269)(0.105)(4.24)$$

$$" = 0.268$$

$$C_D = 0.0242 + \frac{(1.50)}{(14.48)}(0.105)(0.268)^2$$

$$" = 0.0250$$

$$C_{M_{c/4}} = C_{m_{c/4u}} = 0.0181$$

All manometer settings were selected to produce the final dynamic pressure values of 10.0, 20.0, 30.0, 40.0, and 50.0 pounds per square foot. From previous calibration:

$$\frac{q}{q_{ref}} = 1.015$$

As 1.0 pounds per square foot equals 0.496 centimeters of water:

$$q_{ref} = \frac{q}{1.015}(psf)(0.496)$$

The following values were utilized to produce the desired dynamic pressures:

| $q$(psf) | $q_{ref}$ ($cm.H_2O$) |
|---|---|
| 10.0 | 4.89 |
| 20.0 | 9.77 |
| 30.0 | 14.66 |
| 40.0 | 19.55 |
| 50.0 | 24.43 |

Reynolds number, Re, calculations were as follows:

$$R_e = \frac{\rho V c}{\mu}$$

where:

$\rho$ = density (slugs per cubic foot)

$$" = \frac{P}{RT}$$

with:

$P$ = pressure (pounds per square foot)

$R$ = Gas constant = 3092

$T$ = Temperature (degrees Kelvin)

$V$ = velocity (feet per second)

$" = \sqrt{2q/\rho}$

$c$ = chord length

$$\mu = \frac{\mu_o}{(273/T)}.75$$

For example, run number 31:

$q = 30.0$ $\qquad$ $P = 30.11$ mmHg = 2129.7 psf.

$T = 65^oF = 291.3^oK$

$$\rho = \frac{2129.7}{(3092)(291.3)} = 0.002364$$

$$V = \sqrt{(2)(30)/.002364} = 159.31$$

$$\mu = \frac{3.58 \times 10^{-7}}{(273/291.3)}.75 = 3.76 \times 10^{-7}$$

$$Re = \frac{(0.002364)(159.31)(.5)}{(3.76 \times 10^{-7})} = 5.01 \times 10^5$$

All calculations were performed on a Wang Model 360 programmable calculator.

BIBLIOGRAPHY

1. Abbott, I. H., and von Doenhoff, A. E., Theory of Wing Sections, p. 510-511, McGraw-Hill, 1949.

2. Carlson, A., and others, Handbook of Analog Computation, p. 51-54, Electronic Associates, Inc., 1965.

3. Parkhurst, R. C., and Holder, D. W., Wind-Tunnel Technique, Pitman, 1968.

4. Pope, A., Basic Wing and Airfoil Theory, McGraw-Hill, 1951.

5. Pope, A., Wind-Tunnel Testing, 2nd ed., Wiley, 1954.

INITIAL DISTRIBUTION LIST

| | | No. Copies |
|---|---|---|
| 1. | Defense Documentation Center<br>Cameron Station<br>Alexandria, Virginia 22314 | 2 |
| 2. | Library, Code 0212<br>Naval Postgraduate School<br>Monterey, California 93940 | 2 |
| 3. | Chairman, Department of Aeronautics<br>Naval Postgraduate School<br>Monterey, California 93940 | 1 |
| 4. | Professor L. V. Schmidt, Code 57Sx<br>Department of Aeronautics<br>Naval Postgraduate School<br>Monterey, California 93940 | 1 |
| 5. | LCDR S. R. Briggs, USN<br>3513 Londonderry Drive<br>Santa Clara, California 95050 | 1 |

Security Classification

**DOCUMENT CONTROL DATA - R & D**

*(Security classification of title, body of abstract and indexing annotation must be entered when the overall report is classified)*

1. ORIGINATING ACTIVITY *(Corporate author)*

Naval Postgraduate School
Monterey, California 93940

2a. REPORT SECURITY CLASSIFICATION

Unclassified

2b. GROUP

3. REPORT TITLE

Evaluation of an Electronic Wind-Tunnel Balance

4. DESCRIPTIVE NOTES *(Type of report and inclusive dates)*

Master's Thesis; March 1971

5. AUTHOR(S) *(First name, middle initial, last name)*

Steven Russell Briggs

| 6. REPORT DATE | 7a. TOTAL NO. OF PAGES | 7b. NO. OF REFS |
|---|---|---|
| March 1971 | 61 | 5 |

| 8a. CONTRACT OR GRANT NO. | 9a. ORIGINATOR'S REPORT NUMBER(S) |
|---|---|
| b. PROJECT NO. | |
| c. | 9b. OTHER REPORT NO(S) *(Any other numbers that may be assigned this report)* |
| d. | |

10. DISTRIBUTION STATEMENT

Approved for public release; distribution unlimited.

| 11. SUPPLEMENTARY NOTES | 12. SPONSORING MILITARY ACTIVITY |
|---|---|
| | Naval Postgraduate School<br>Monterey, California 93940 |

13. ABSTRACT

The three-component electronic wind-tunnel balance installed in the 3.5 by 5.0 foot subsonic tunnel of the Aeronautics Department of the Naval Postgraduate School was evaluated for system problem areas. The nonlinear output of the reluctance gage transducers was analyzed and linearized using diode function-generating circuitry. A static calibration was conducted to confirm the linearity of the circuits. Evaluation of the balance system under operating conditions pointed out other areas for future investigation. Aerodynamic support tares must be determined, an improved pitch angle drive system is required, a mechanical damping system should be installed, and the balance must be isolated from its existing elastic platform.

| 14 KEY WORDS | LINK A | | LINK B | | LINK C | |
|---|---|---|---|---|---|---|
| | ROLE | WT | ROLE | WT | ROLE | WT |
| Wind-tunnel balance | | | | | | |
| Linearization technique | | | | | | |
| Diode function generating circuit | | | | | | |
| Reluctance gage | | | | | | |

Thesis 126780
B8083 Briggs
c.1 Evaluation of an
electronic wind-tunnel
balance.